Broadband Dielectric Spectroscopy on the Molecular Dynamics in Dendritic Model Systems†

A. Huwe,*,‡ D. Appelhans,§ J. Prigann,‡ B. I. Voit,§ and F. Kremer‡

Department of Physics, University of Leipzig, Linnéstrasse 5, D-04103 Leipzig, Germany, and Institute of Polymer Research, Hohe Strasse 6, D-01069 Dresden, Germany

Received December 30, 1999

ABSTRACT: Broadband dielectric spectroscopy (10^{-1}−10^{7} Hz) is employed to study the molecular dynamics in a set of dendritic poly(ether amide)s involving three generations. In the amorphous systems a dynamic glass transition is found which scales well with calorimetric data. Additionally, one broadened or two frequency separated secondary relaxations are detected. They are assigned to local fluctuations of the ester, amide, and Boc-protected amine groups. This interpretation is confirmed by IR spectroscopy and calculations of the dipole moment of the fluctuating moieties.

Introduction

Dendritic macromolecules belong to one of the most interesting fields in polymer chemistry during the past years. These include dendrimers[1] and hyperbranched polymers.[2] The unique class of dendrimers is characterized by a perfectly branched, three-dimensional structure originating from a core molecule with a branching point at each monomer unit (AB_2 monomer) and a large number of chain ends. Such structures have been prepared by two different strategic approaches: divergent growth[3] (from the inside out) and convergent growth[4] (from the outside in). Hyperbranched polymers are synthesized in a one-step reaction using a high functionality monomer of the type AB_x. This results in a highly branched, irregular structure. In addition to the well-examined syntheses of these macromolecules, studies have also focused on the investigation of their chemical and physical properties.

Dendritic macromolecules exhibit new properties resulting from their unusual architecture. In comparison to linear polymers, for example, the melt viscosity is considerably lower for hyperbranched polymers.[5] It can also be shown that the relationship between hydrodynamic volume and molar mass is different between the linear and the hyperbranched polymers.[2] The investigations of glass transition temperature (T_g) in hyperbranched polymers have correlated T_g's to the number of monomer units, number of chain end, molecular weight, and chain end composition.[6,7] Investigations of the physical properties of dendrimers have been focused on minima or maxima in density,[8] intrinsic viscosity, refractive index, and the unusual solubility characteristics.[9] Further investigations are related to the T_g of different dendrimers based on differential scanning calorimetry (DSC) measurements. In general, T_g increases with molar mass up to a certain limit, above which the T_g remains practically constant.[10] T_g values go up with increasing polarity of the end groups.[7] Stutz[11] summarized in a theoretical treatment of the T_g for dendritic polymers that the T_g is mainly a function of the generation number of the branching step but independent of the number branching arms per molecule. Therefore, the T_g is also independent of the molar mass of the whole molecule. Additional, the rigidity of the backbone (= repeating branching units) and the nature of the terminal group influence the T_g of dendritic polymers considerably. Further comparison of the glass transition temperature between linear and dendritic polymers gave that only a comparatively small difference of the T_g exists. This fact could also be shown by Fréchet et al.[6]

Dielectric spectroscopic investigations examine and explain different molecular dynamic processes (α-, β-, γ-, and δ-relaxation) of dendritic polymers. For example, dielectric spectroscopy on hyperbranched polyester[12] with the same backbone but different terminal groups allows to determine glass transitions (α-relaxations) which agreed well with those obtained in DSC measurements and dynamic mechanical analyses. It was also possible to distinguish the different β- and γ-relaxation processes for the terminal ester and hydroxy groups. Stühn et al.[13,14] applied dielectric spectroscopy on carbosilane dendrimers with flexible perfluorinated and mesogenic end groups to study the possible smectic and nematic state and their transitions of these highly flexible dendritic macromolecules. Besides the dielectrical analyzed carbosilane dendrimers, an example for ester-terminated, amide-based dendrimers was as well presented by Emran et al.[15] The identification of glass transitions was characterized by the Vogel−Fulcher−Tammann behavior. The dendrimers showed also secondary relaxations with an Arrhenius type temperature dependence and activation energies between 37.7 and 85.8 kJ/mol. In summary, the application of dielectric spectroscopy on dendrimers provided a deeper understanding of molecular dynamics and phase transitions of superstructures. In this paper the results of dielectric spectroscopy for dendritic poly(ether amide)s[16] (Table 1) are presented which offered partly separated β-relaxation processes for ester and amide groups. Further these materials can be considered as molecular modular system of larger dendritic poly(ether amide)s based on the repeating monomer 5-(2-aminoethoxy)isophthalic acid[17] to study specific molecular dynamics which are not revealed directly in larger dendritic poly(ether amide)s.

† Dedicated to Prof. Dr. Jürgen Springer, TU Berlin, on the occasion of his 65th birthday.

‡ University of Leipzig.

§ Institute of Polymer Research.

10.1021/ma9921854 CCC: $19.00
Published on Web 04/21/2000

Table 1. Chemical Structure and Glass Transition Temperature of the Investigated Compounds (Different Dendritic Molecules)[a]

Compound	T_g temperature in K	Denotation
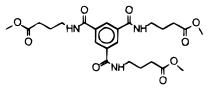		**G0**
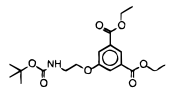	266.5	**Boc-G1**
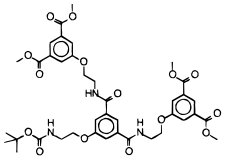	337.5	**Boc-G2**
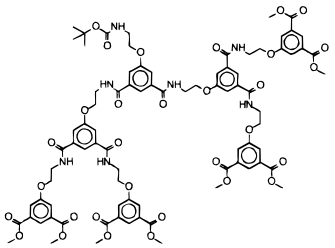	357.0	**Boc-G3**
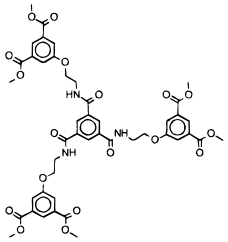	355.5	**G1-Tri**

[a] The glass transition temperatures were determined by DSC measurements (scanning rate: 20 K/min).

Experimental Section

Details of the synthesis and characterization of the dendrons Boc-G1, Boc-G2, and Boc-G3 were given previously.[16] The synthesis and characterization of G0 and G1-Tri are presented in a forthcoming paper.[17] To prepare the samples, the dendritic materials were heated to approximately 150 °C. The melt was kept between two brass electrodes with 50 μm glass fiber spacers. The sample diameter was 10 mm. Isothermal dielectric spectra starting with the highest temperature were measured in the frequency range from 10^{-1} to 10^{7} Hz. For this purpose a Solatron-Schlumberger frequency response analyzer FRA 1260 in combination with a Novocontrol active sample cell BDC-S was used. The relative accuracy is 5% in ϵ', and the resolution in tan(δ) is better than 10^{-3}. The sample temperatures are controlled in a nitrogen gas jet (Quatro, Novocontrol GmbH) with a stability better than 0.05 K. Details of the setup may be found in ref 18.

Results and Discussion

Isothermal data of the dielectric loss ϵ'' are fitted to a superposition of one or two relaxation functions according to Havriliak−Negami (HN) and a conductivity contribution.[19]

$$\epsilon'' = \frac{\sigma_0}{\epsilon_0}\frac{a}{\omega^s} - \mathrm{Im}\left[\frac{\Delta\epsilon}{(1+(i\omega\tau)^{\alpha})^{\gamma}}\right] \qquad (1)$$

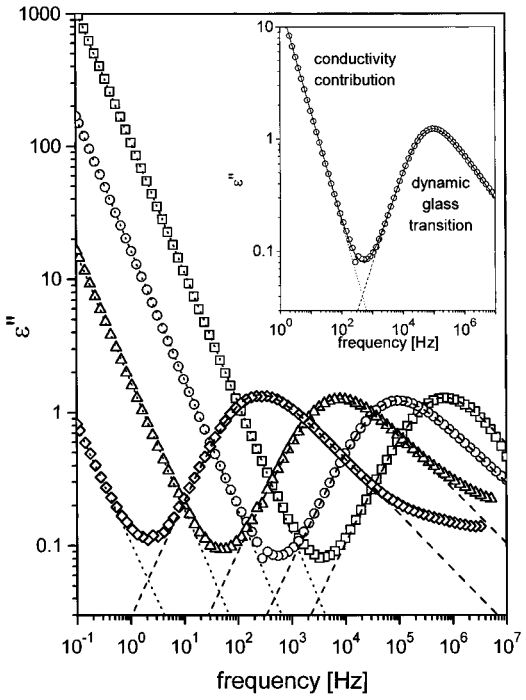

Figure 1. Dielectric loss ϵ'' versus frequency of the first-generation dendron Boc-G1 for four different temperatures: 315 K (squares), 305 K (circles), 295 K (triangles), and 285 K (diamonds). The inset shows the deconvolution of the data: dashed line, HN relaxation; dotted line, conductivity contribution; solid line, resulting sum. Deviations at higher frequencies are caused by a second relaxation (β-relaxation).

In this notation one relaxation process is assumed. ϵ_0 is the vacuum permittivity, σ_0 the dc conductivity, and $\Delta\epsilon$ the dielectric strength. α and γ describe the symmetric and asymmetric broadening of the relaxation peak. The exponent s equals one for Ohmic behavior, deviations ($s < 1$) are caused by electrode polarization or Maxwell−Wagner polarization effects, and a is a factor having the dimension s^{1-s}. From the fits according to eq 1 the relaxation rate $1/\tau_{max}$ can be deduced which is given at the frequency of maximum dielectric loss ϵ'' for a certain temperature.

The samples show different relaxation processes: One is present in the observed frequency range at temperatures above the calorimetric glass transition temperature. We assign this process to the α-relaxation. Figure 1 shows the dielectric spectra for Boc-G1 at different temperatures above T_g and the deconvolution of the data. The deviation between the data and the fit at higher frequencies is caused by a second relaxation process. Sample G0 does not show either a calorimetric glass transition or a dynamic glass transition. Figure 2 shows the relaxation rate of the dynamic glass transition as a function of inverse temperature. The data have a characteristic temperature dependence according to Vogel−Fulcher−Tammann (VFT dependence):[20]

$$\frac{1}{\tau} = \frac{1}{\tau_0}\exp\left(\frac{-DT_0}{T-T_0}\right) \qquad (2)$$

where D is the fragility parameter and T_0 the Vogel temperature. The fits describe the experimental results very well. The dynamic glass transition temperature is conventionally defined as the temperature, where the relaxation time is 100 s.[21,22] By extrapolating the VFT fit to $\log(1/\tau) = -2$, one obtains for the dynamic glass

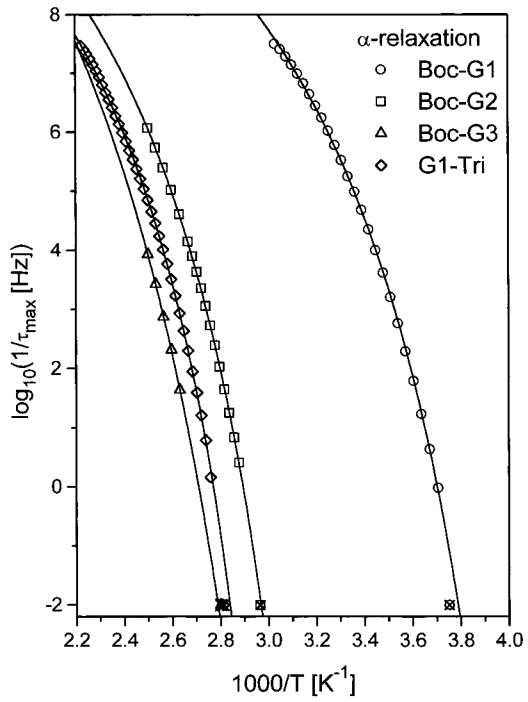

Figure 2. Relaxation rate of the α-relaxation versus inverse temperature for Boc-G1 (circles), Boc-G2 (squares), Boc-G3 (triangles), and G1-Tri (diamonds). The error bars are smaller than the size of the symbols. The lines are fits according to the VFT equation (2). The symbols marked by a cross indicate the respective calorimetric glass transition. They fit well with the extrapolated temperature at a relaxation rate of the dynamic glass transition of 10^{-2} Hz.

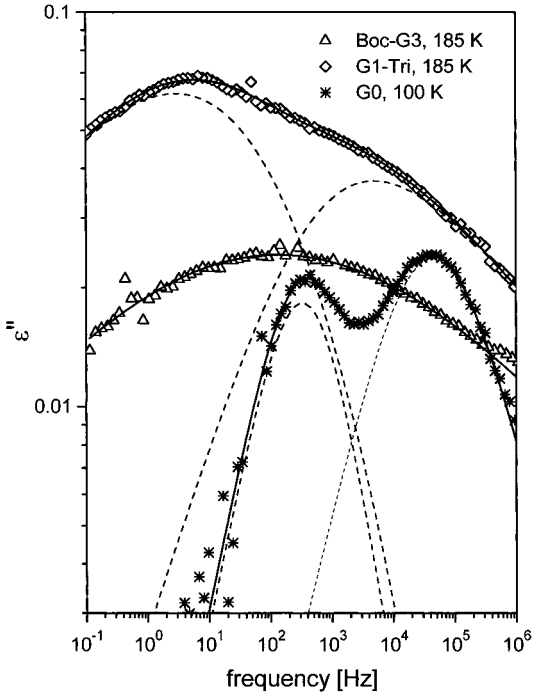

Figure 3. Dielectric loss ϵ'' versus frequency of the third-generation dendron Boc-G3 at 185 K (triangles), of G1-Tri at 185 K (diamonds), and of G0 at 100 K (stars). The lines represent HN fits to the data. The dashed lines are the fits of each relaxation process in G0 and G1-Tri, and the solid line is the resulting sum.

transition temperature for Boc-G1, Boc-G2, Boc-G3, and G1-Tri 264, 337, 359, and 352 K, respectively. These values are in good agreement with the calorimetric data as shown in Table 1. The largest deviation is only 2.5 K. In Figure 2 the symbols marked by a cross represents the calorimetric data.

At lower temperatures all dendritic materials show β-relaxations. Figure 3 shows the dielectric data of the tridendron G1-Tri and of the third generation dendron Boc-G3 at 185 K and of G0 at 100 K. The dielectric spectra of Boc-G1, Boc-G2, and Boc-G3 can be fitted with one relaxation process whereas in G1-Tri and G0 two processes are observed. Figure 4 shows the relaxation rates of the β-relaxation of all compounds. The activation energies of the β-processes in G0 range between 16 and 20 kJ/mol which are significantly lower than the values of ester-terminated amide-based dendrimers.[15] In contrast, the secondary relaxations in the amorphous materials have activation energies which vary between 35 and 44 kJ/mol. These values are slightly lower compared to the values of poly(amide) dendrimers.[15] Furthermore, the β-relaxation of G0 differs strongly from the other ones. They are much more faster (see Figure 4), and their peaks are well separated (see Figure 3). This can be explained by the fact that G0 is in the crystalline phase, but the other dendritic materials are in the amorphous state. The two relaxation processes are assigned to local fluctuations of the ester and the amide group in the G0 molecule. This assignment can also be done for G1-Tri, which shows two β-processes and has ester and amide groups as well. To confirm this interpretation the electric dipole moment, which can be calculated from the dielectric strength $\Delta\epsilon$ of the experimental data, can be compared to the theoretical value obtained by static computer simulations. Neglecting the

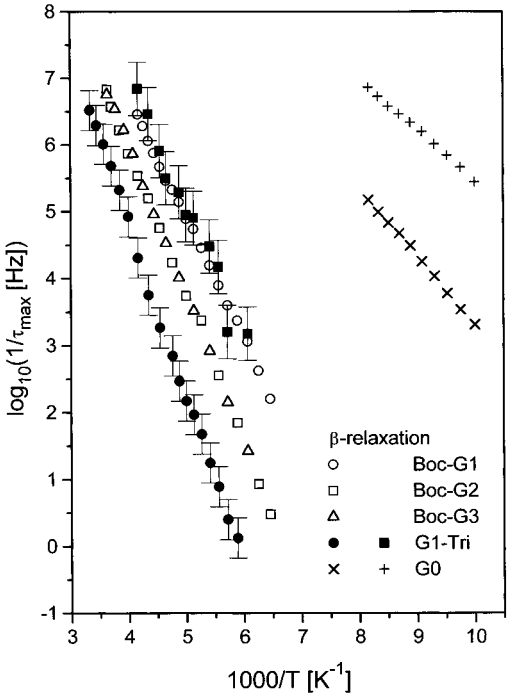

Figure 4. Relaxation rate of the β-relaxation versus inverse temperature for Boc-G1 (open circles), Boc-G2 (open squares), Boc-G3 (open triangles), G1-Tri (solid circles and solid squares), and G0 (crosses). If not indicated otherwise, the error bars are smaller than the size of the symbols.

dipole−dipole interaction, the relation between the dielectric strength $\Delta\epsilon$ and the dipole moment μ is

$$\Delta\epsilon = n \frac{\mu^2}{3kT\epsilon_0} g_{KF} \qquad (3)$$

Table 2. Dipole Moment As Determined from the Strength of the β-Relaxation According to Eq 3[a]

sample	dipole moment [10^{-30} A s m]	sample	dipole moment [10^{-30} A s m]
Boc-G1	8.3 ± 1.7	G1-Tri	4.2 ± 1.0
Boc-G2	5.4 ± 1.1	G0	5.6 ± 1.2
Boc-G3	6.5 ± 1.3		

[a] From molecular simulations for the ester group a dipole moment of $(4.2 \pm 1.7) \times 10^{-30}$ A s m and for the amide group $(6.0 \pm 1.2) \times 10^{-30}$ A s m are obtained.

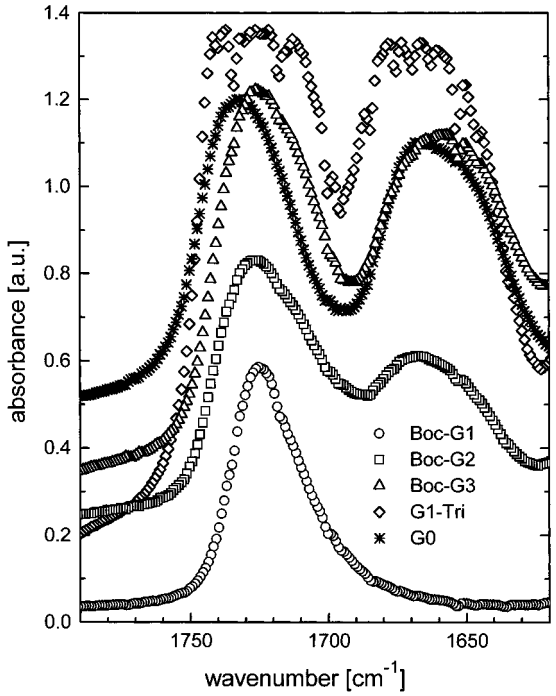

Figure 5. Absorbance for Boc-G1 (circles), Boc-G2 (squares), Boc-G3 (triangles), G1-Tri (diamonds), and G0 (stars) in dependence on the wavenumber at a temperature of 140 °C.

n is the dipole density, and g_{KF} is the Kirkwood–Froehlich factor which describes dipole–dipole correlations. It is assumed that the ester, amide, and Boc-protected amine groups contribute to the dipole density. The theoretical values for the dipole moment are calculated with the program Cerius[2]. Table 2 shows the calculated dipole moments for all samples. Within the errors there is a consistency between the experimental data and the theoretical values for the ester group ($(4.2 \pm 1.7) \times 10^{-30}$ A s m) and for the amide group ($(6.0 \pm 1.2) \times 10^{-30}$ A s m). The latter one shows a higher dipole moment than the ester group. Therefore, the amide groups contribute more to the dielectric strength although they are less in number. Boc-G1 has a slightly larger dipole moment compared to the other materials and compared to the theoretical results, but it has also a significantly lower glass transition temperature. This may be caused by a different configuration or packing of the molecules. If the molecular assignment of the β-processes holds, it is difficult to understand why Boc-G1, Boc-G2, and Boc-G3 show only one β-process.

In addition, infrared spectra were taken. Figure 5 shows that all samples except Boc-G1 have two absorption bands for the carbonyl group, which is present in all dielectric active groups of the dendritic molecules. If these two bands are assigned to the ester and the amide group, it has to be concluded that the Boc-protected amine group in Boc-G1 is similar to an ester group. The β-relaxation of Boc-G1 in Figure 4 is assigned to the fluctuations of the ester group and coincides with the corresponding fluctuations in G1-Tri. The slower β-process in G1-Tri and of course in G0 originates from the amide groups. In Boc-G2 and Boc-G3 the relaxation process of the ester and the amide groups merge into one broad process whose relaxation rate lies between those two of G1-Tri (see Figure 4).

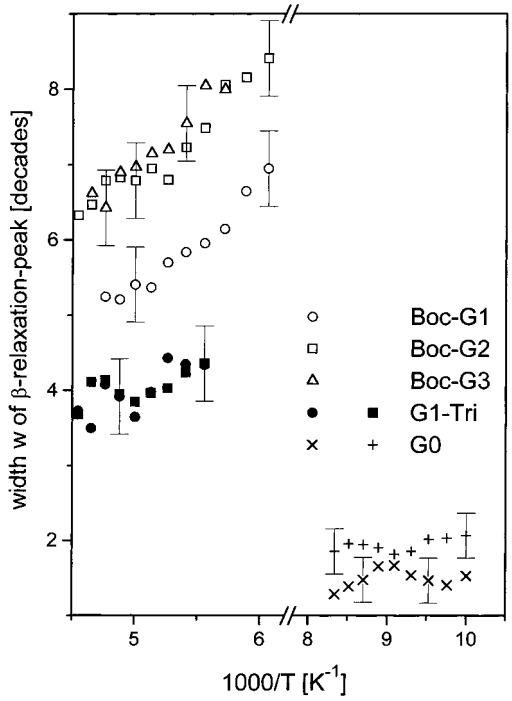

Figure 6. Width w of the relaxation peak (full width at half peak maximum) as a function of inverse temperature for Boc-G1 (open circles), Boc-G2 (open squares), Boc-G3 (open triangles), G1-Tri (solid circles and solid squares), and G0 (crosses).

Figure 6 shows the width w of the relaxation peak (full width at half peak maximum) as a function of temperature for all examined materials. G0 with its crystalline structure has a narrow peak (being in its width close to an ideal Debye relaxation which has $w = 1.14$). In the amorphous state the peaks broaden dramatically even if the molecule, like G1-Tri, has a high symmetry. For Boc-G2 and Boc-G3 a splitting into two β-relaxations cannot be observed.

Conclusion

The molecular dynamics of several dendritic low-molecular-weight molecules was studied by broadband dielectric spectroscopy. For the amorphous materials an α-relaxation (dynamic glass transition) was found. The dielectrically determined glass transition temperatures agree well with calorimetrically measured values. For the β-relaxations a molecular assignment to ester, amide, and Boc-protected amine groups is suggested. The observed relaxation strength fits well to the results obtained by numerical calculations of the involved dipole moments.

References and Notes

(1) Tomalia, D. A.; Naylor, A. M.; Goddard, A. M. *Angew. Chem.* **1990**, *102*, 119. Newkome, G.; Moorefield, C. N.; Vögtle, F. *Dendritic Molecules–Concepts, Syntheses, Perspective*; VCH: Weinhein, 1996. Bosman, A. W.; Janssen, H. M.; Meijer, E.

W. *Chem. Rev.* **1999**, *99*, 1665. Newkome, G. R.; He, E.; Moorefield, C. N. *Chem. Rev.* **1999**, *99*, 1689.
(2) Flory, P. J. *Principles in Polymer Chemistry*; Cornell University Press: Ithaca, NY, 1953. Fréchet, J. M. J.; Hawker, C. J. Synthesis and Properties of Dendrimers and Hyperbranched Polymers. In *Comprehensive Polymer Science*; Second Supplement; Aggarwal, S. L., Russo, S., Eds.; Elsevier Science Ltd.: Oxford, 1996; p 71 and references therein.
(3) Newkome, G. R.; et al. *J. Org. Chem.* **1992**, *57*, 358.
(4) Hawker, C. J.; Fréchet, J. M. J. *J. Am. Chem. Soc.* **1990**, *112*, 7638.
(5) Hawker, C. J.; Farrington, P. J.; McKay, M. E.; Wooley, K. L.; Frechet, J. M. J. *J. Am. Chem. Soc.* **1995**, *117*, 4409.
(6) Wooley, K. L.; Fréchet, J. M. J.; Hawker, C. J. *Polymer* **1994**, *35*, 4489.
(7) Kim, Y. H.; Beckerbauer, R. *Macromolecules* **1994**, *27*, 1968.
(8) Tomalia, D. A.; Naylor, A. M.; Goddard, A. M. *Angew. Chem., Int. Ed. Engl.* **1990**, *29*, 138.
(9) Mourey, T. H.; Turner, S. R.; Rubinstein, M.; Frechet, J. M. J.; Hawker, C. J.; Wooley, K. L. *Macromolecules* **1992**, *25*, 2401.
(10) Wooley, K. L.; Hawker, C. J.; Pochan, J. M.; Frechet, J. M. J. *Macromolecules* **1993**, *26*, 1514.
(11) Stutz, H. *J. Polym. Sci., Part B: Polym. Phys.* **1995**, *33*, 333.
(12) Malmström, E.; Liu, F.; Boyd, R. H.; Hult, A.; Gedde, U. W. *Polymer* **1997**, *38*, 4873.
(13) Trahasch, B.; Frey, H.; Lorenz, K.; Stühn, B. *Colloid Polym. Sci.* **1999**, *277*, 1186.
(14) Trahasch, B.; Stühn, B.; Frey, H.; Lorenz, K. *Macromolecules* **1999**, *32*, 1962.
(15) Emran, S. K.; Newkome, G. R.; Weis, D. W.; Harmon, J. P. *J. Polym. Sci., Part B: Polym. Phys.* **1999**, *37*, 2025.
(16) Voit, B. I.; Wolf, D. *Tetrahedron* **1997**, *53*, 15535.
(17) Appelhans, D.; Komber, H.; Voigt, D.; Häussler, L.; Voit, B. *Macromolecules*, in preparation.
(18) Kremer, F.; Boese, D.; Maier, G.; Fischer, E. W. *Prog. Polym. Sci.* **1989**, *80*, 129.
(19) Havriliak, S.; Negami, S. *J. Polym. Sci., Part C* **1966**, *14*, 99.
(20) Vogel, H. *Phys. Z.* **1921**, *22*, 645. Fulcher, G. S. *J. Am. Chem. Soc.* **1925**, *8*, 339. Tammann, G.; Hesse, G. *Anorg. Allg. Chem.* **1926**, *156*, 245.
(21) Donth, E. *Glasübergang*; Akademie Verlag: Berlin, 1981.
(22) Angell, C. A. *Science* **1995**, *267*, 1924.

MA9921854